Preloading of a hydraullic fill for foundation of LNG tanks

Fernando Román, Technical University of Madrid (UPM), Spain, fernando.roman@upm.es
Rafael Jimenez, Technical University of Madrid (UPM), Spain rafael.jimenez@upm.es
Julio C. García Suarez, Enagás S.A., Spain, jcgarcia@enagas.es
Ana Coz, Eng. Geologist, Spain, anacoz@gmail.com

ABSTRACT

A liquefied natural gas (LNG) plant is currently being constructed on a hydraulic fill in El Musel Port (Gijon, Northern Spain). The hydraulic fill is mainly composed of marine sands dredged from nearby locations, and it was placed on site using rainbow and pipeline discharge and the bottom dump method. Preloading was selected among several alternatives as the ground improvement method employed to reduce settlements of the LNG tanks. This paper presents the results of the geotechnical characterization campaign conducted at the site (SPT, CPTU, DPSH) and at the laboratory. In addition, the main features of the preloading employed are presented, as well as the results of the monitored settlements (both during preloading and during the construction of the tanks).

1. INTRODUCTION

In a recent extension to El Musel Port (Gijon, northern Spain), almost three kilometers of new docks have been constructed, as well as 145 hectares of new surface behind the docks. Most of this new (reclaimed) land has been constructed by means of hydraulic fills with dredged material. The volume of fill material is above 32 million cubic meters. Gijon Port Authorities (APG) developed in 2009 a new surface of 260.000m2, of which 220.000m2 were occupied by ENAGAS (the Spanish Technical Manager of the Gas system and Common Carrier for the high pressure gas network) to build a regasification plant of Liquefied Natural Gas (LNG). (For a review of similar uses of hydraulic fills, see Whitman (1970).)

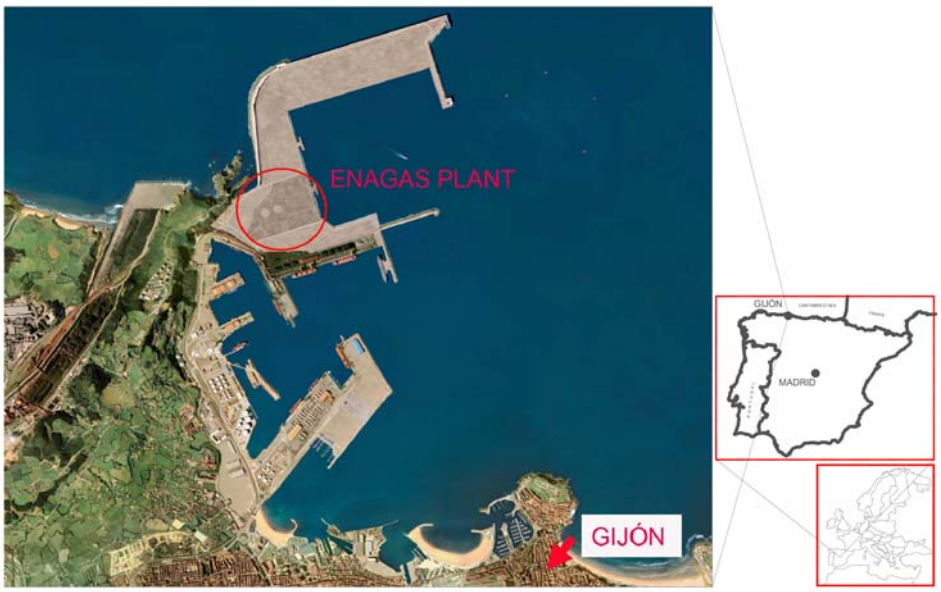

Figure 1: Location of Enagás Plant

The main structures in the new regasification plant are two tanks for storage of the LNG. Their dimensions are 78,2 m of diameter and 50,5 m of maximum height, with an storage capacity of 150.000 m3 each. The tanks have an exterior ring of pre-stressed concrete of 80 cm thickness, and a concrete dome reinforced with a steel structure. The foundation mat has a diameter of 82,4 m and a thickness of 0,70 m, that is increased to 1,2 m under the 5,4 m wide area below the exterior concrete ring. The service load transmitted by the tank is 200 kPa, and the load during the hydraulic test is 285 kPa.

Before the port extension, the sea bed was located between -15 and -20 m O.D.. Between 2006 and 2008, the APG started to fill the "Enagas area" with approximately 600.000 m3, which elevated the sea bed up to -8 m O.D. in some points in the southwest corner. During 2009, an additional 4,5 million m3 have been filled using two dredges and the rainbow discharge, bottom dump, and pipeline discharge methods (Lee et al., 1999). The final height of the fill is +6,40 m O.D., which means that the fill thickness ranges from 21

to 26 meters. The materials below the fill include thin Quaternary layers of dense sands and gravels underlayed by bedrock composed of limestone, marls, and quartzite.

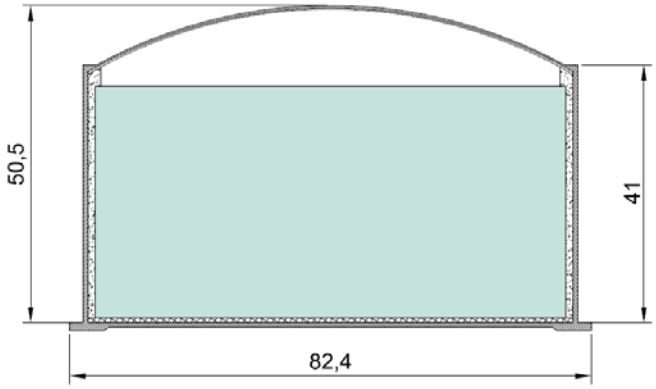

Figure 2: Schematic cross-section of the LNG storage tank

2. GROUND INVESTIGATION

The following works were performed:

- 25 boreholes (rotary core drilling), with "undisturbed" samples taken every 3 m and with SPT tests conducted immediately after each sample taken.
- 55 continuous dynamic penetration tests (DPSH)
- 2 continuous BORROS dynamic penetration tests (DPH)
- 23 cone penetration tests with pore pressures measurement (CPTU), and with 6 dissipation tests.
- 6 seismic cone tests (SCPTU) with measurement of wave velocities
- 10 exploratory ditches.

Even though the position of the boreholes and tests conducted was mainly selected depending on the position of the facilities in the plant, it was also intended that the overall dataset would allow a good characterization of the site.

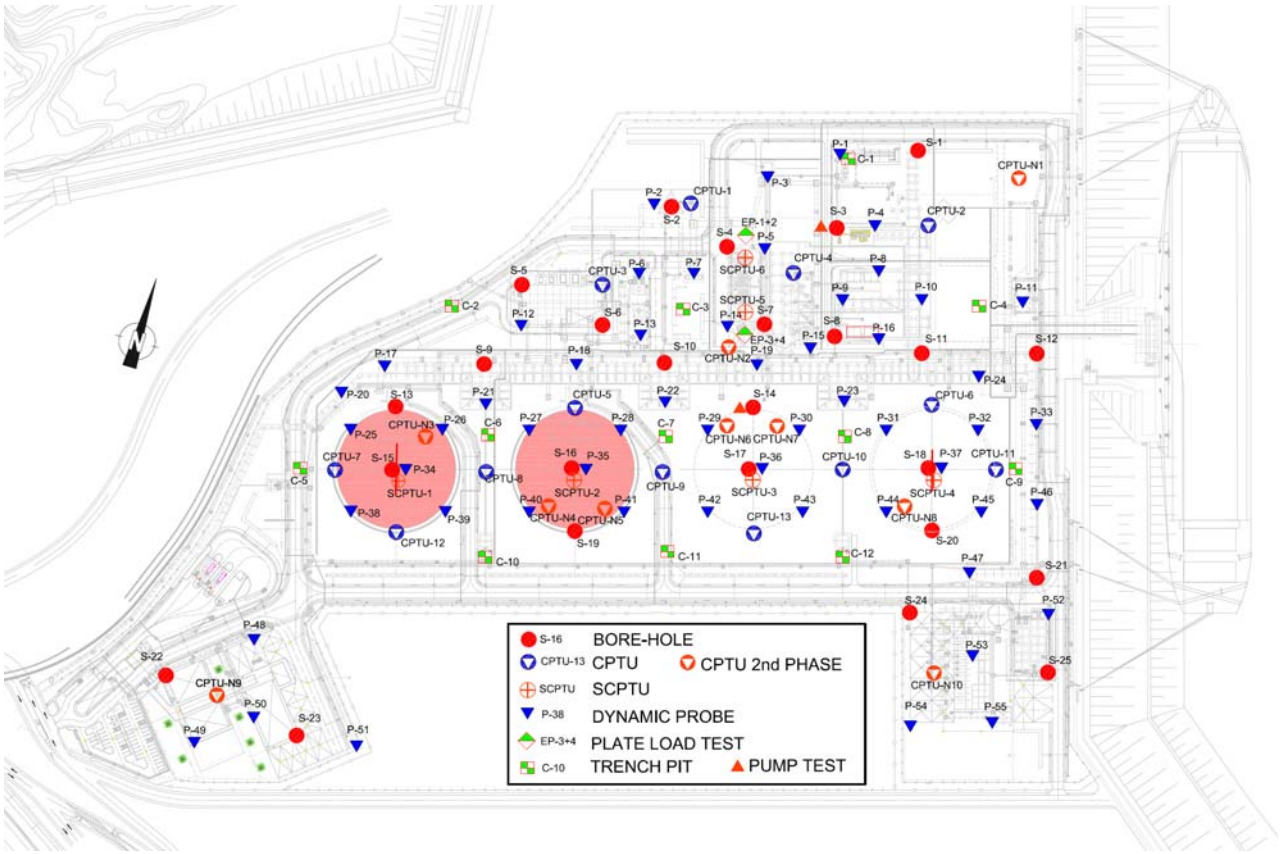

Figure 3: Lay out of the site characterization program

3. GEOTECHNICAL CHARACTERIZATION

3.1. Composition, granulometry, plasticity

The fill materials are sands (with variable silt content) whose particles are mainly composed of shell fragments (50 to 60%; see Photo 1). Because of such composition, tests were conducted to study whether there were variations (due to particle breakage) after the material was compacted (Modified Proctor).

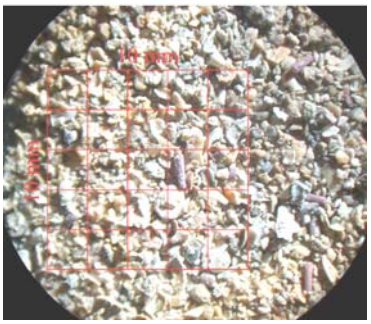

Photo 1: Sand sample (size of the grid is 10 mm)

Figure 4 shows the granulometric curves of all the samples taken from the borehole samples. In most cases, the fines content (measured as particles smaller than 0,080mm) is below 30%. Figure 5 shows the fines content as a function of depth. Particles smaller than 0,4mm are always non-plastic.

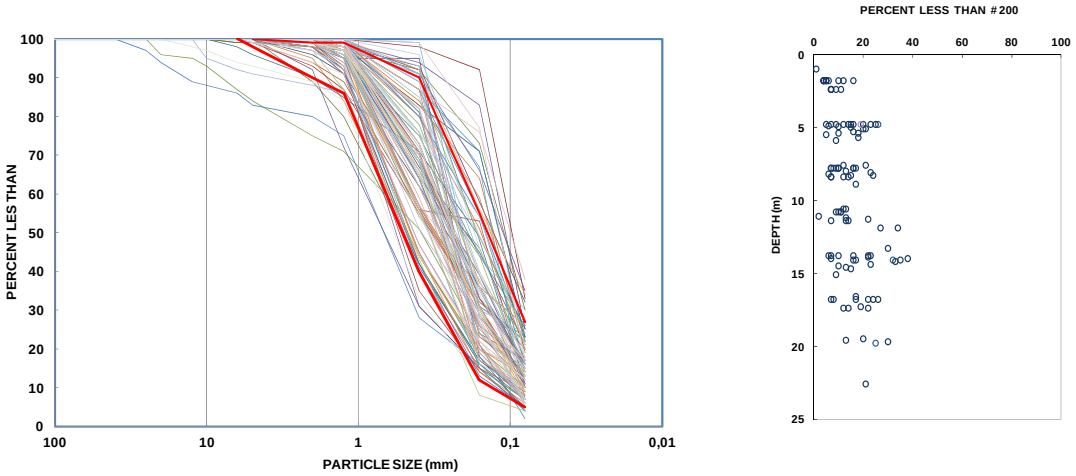

Figures 4 & 5: Size analysis curves and distribution of passing 0,080 mm with depth

3.2. Dynamic penetration resistance (SPT, DPSH and BORROS).

SPT tests were conducted inside the boreholes taking special care so as to avoid the heave of the bottom once that the sample was extracted before the test. SPT test results are shown in Figure 6 (a red line indicates the average of tests at each depth). Table 1 lists representative SPT values for each depth.

Table 1 :Representatives values of SPT

Depth (m)	N_{30}SPT
(Over phreatic level)	7 - 15
3,5 a 8,5	3 - 7
8,5 a 13	4 - 9
13 a 18	6 – 14
18 a 22	8 – 17
22 a 24	15 -23

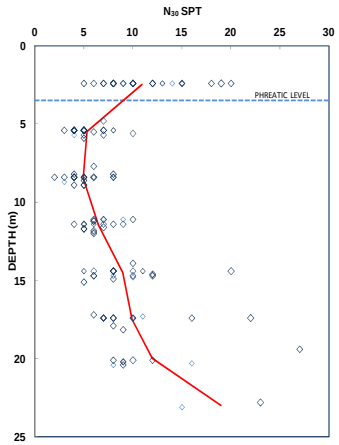

Figure 6.- SPT versus depth

Dynamic penetration tests (DPSH) have been employed to estimate the density of the sands at the site. Figure 7 shows their evolution with depth, and Table 2 lists representative values. To serve as a contrast, two BORROS dynamic penetration tests were conducted as well.

Table 2: Representatives values of DPSH

Depth (m)	**N_{20} DPSH**
(Over phreatic level)	5 – 11
3,5 a 8	1 – 4
8 a 13	3 – 8
13 a 16	6 – 10
16 a 18	8 – 15
18 a 24	12 -18

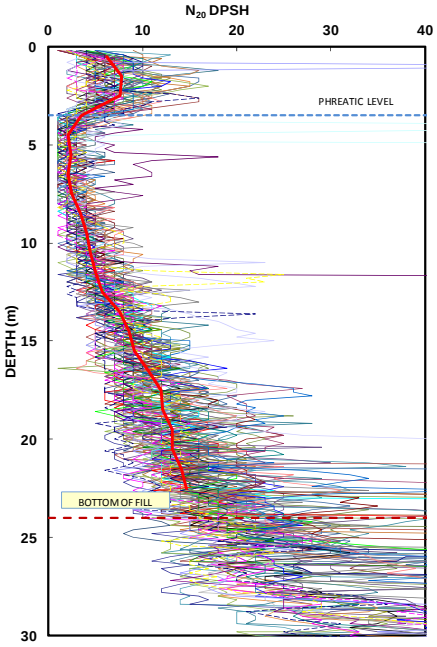

Figure 7: N_{20} DPSH versus depth

The following correlation could be established:

$$N_{20\,DPSH} = 0{,}67 \cdot N_{20\,BORROS}$$

We have also correlated the results of DPSH and SPT tests (for SPT, with the normalization to obtain $N_{1(60)}$.) In DPSH tests, the rods have a somewhat greater lateral friction than in SPT and, therefore, the energy loss is greater. At shallow depths, the energy loss due to lateral friction is small and, therefore, similar in both tests; that produces SPT values approximately 1,5 times the DPSH values (30cm are introduced in SPT vs. 20cm in DPSH). With depth, both values become similar, and that is why in the SPT $N_{1(60)}$ values there is a correction for rod length (C_R=0,75) but there is not a similar correction for the DPSH. Figure 8 shows the relationship between SPT and DPSH values with depth (**$N_{1(60)}$ /N_{20}**), and Table 3 shows representative value of such ratio. (Note that at depths indicated with (*) –i.e., between depths 3,5 and 8m-- there is a greater dispersion of values because both SPT and DPSH are quite small).

*Table 3: Representatives values of **$N_{1(60)}$ /N_{20} DPSH***

Depth (m)	**$N_{1(60)}$ /N_{20} DPSH**
(Over phreatic level)	1,2 -2,2
3,5 a 7	1,2 – 2,2 (*)
7 a 10	1 – 1,7 (*)
10 a 24	0,8 -1,2

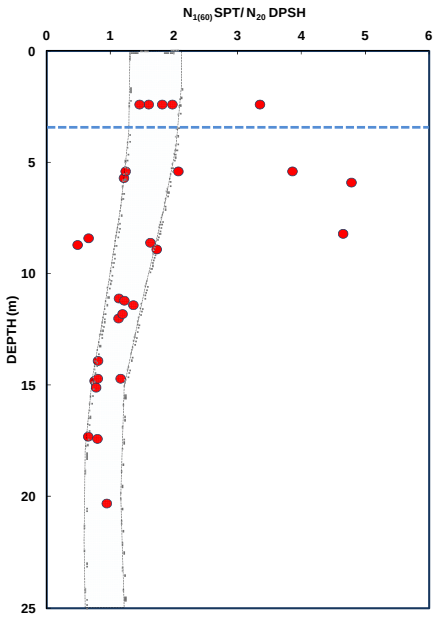

Figure 8: $N_{1(60)}$ /N_{20} DPSH versus depth

3.3. Static Cone Penetration Tests (CPTU)

CPTU has been widely employed for characterization of hydraulic fills (see e.g., Lee (2001); Na et. al (2005)). The CPT penetration resistance (as given by tip resistance and sleeve friction) are shown in Figs 9 and 10.

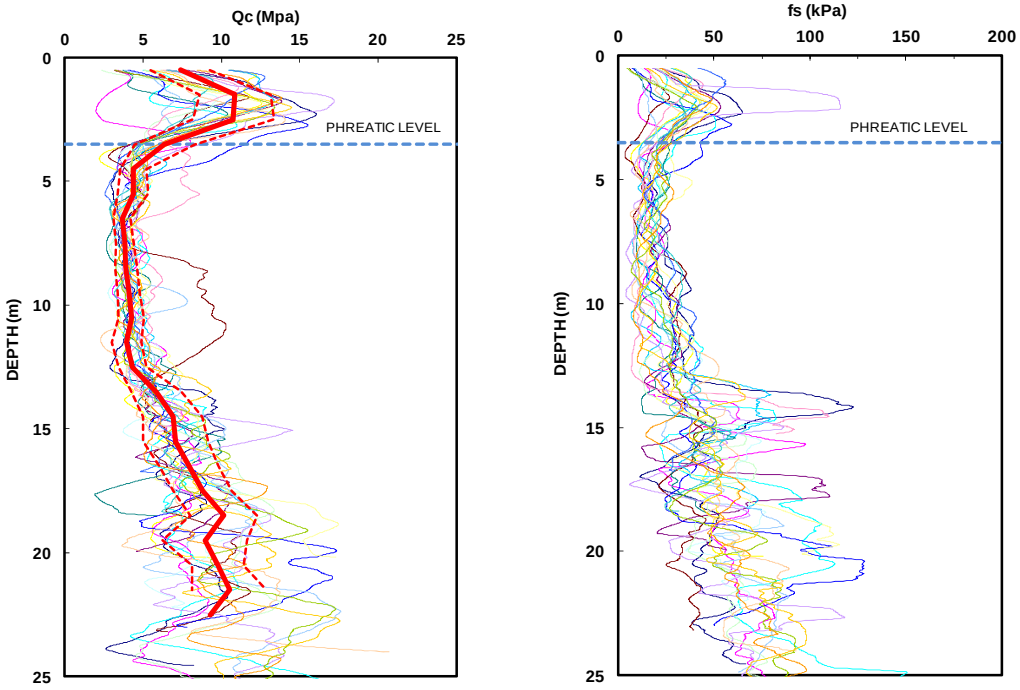

Figures 9 & 10: Tip resistance and sleeve friction vs. depth.

Table 4 shows the representative values that correspond to the selected area in Figure 9.

Table 4: Representative values of Q_C

Depth (m)	Qc (MPa)
(Over phreatic level)	7 - 14
3,5 a 13	3 - 6
13 a 16	4 – 10
16 a 24	6 – 13

If we correlate the static penetration (tip resistance, Qc) with the dynamic penetration resistance (SPT or DPSH) (see e.g., Robertson et al. (1983), we obtain the results shown in Figures 11 to 13. (Table 5 summarizes results.) We could also establish the following correlation:

$$Q_c = (0{,}8\ a\ 1) \cdot N_{1(60)}$$

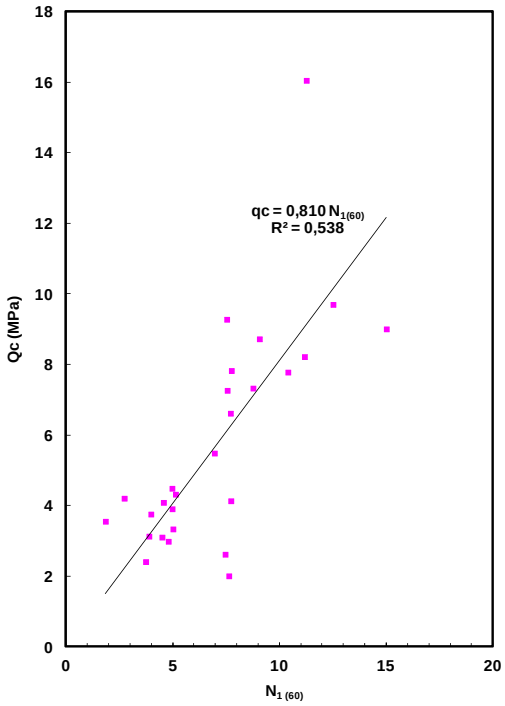

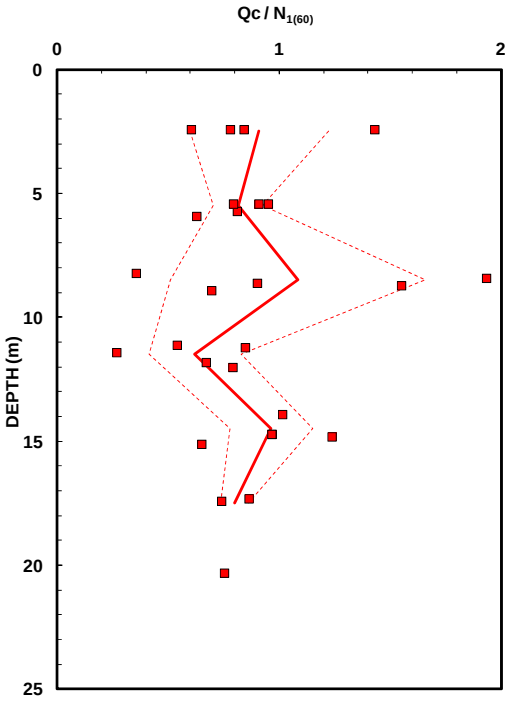

Figures 11 &12: Correlation between Qc and $N_{1(60)}$, and $Qc/N_{1(60)}$ ratio versus depth.

Table 5 : Representative values of Q_C/N_{20} DPSH

Depth (m)	Qc/N_{20}DPSH
(Over phreatic level: 3,50 m)	1,0 -1,6
3 a 7	1,5 – 2 (*)
7 a 10	1,0 – 1,6
10 a 24	0,7 - 0,9

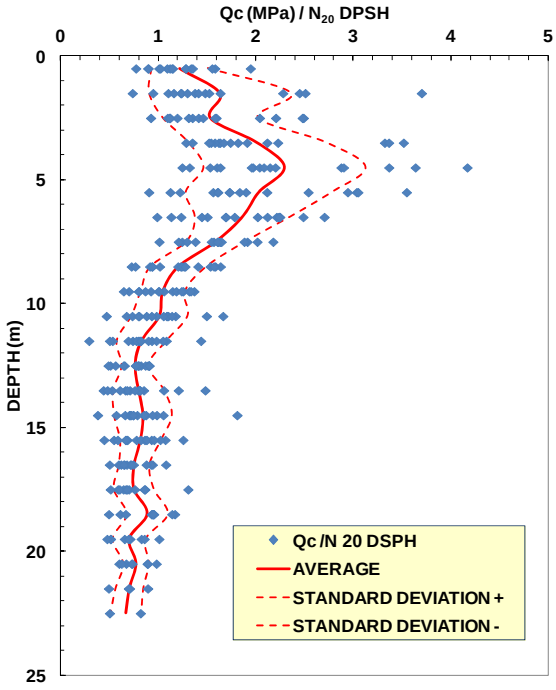

Figure 13: Ratio Qc/N_{20}DPSH versus depth.

3.4. Seismic wave velocities measured in SCPTU

Seismic wave velocities measured with the SCPTU tests are shown in Figure 14. Figure 15 shows the relationship between velocity of S-waves and static cone tip penetration resistance (Qc).

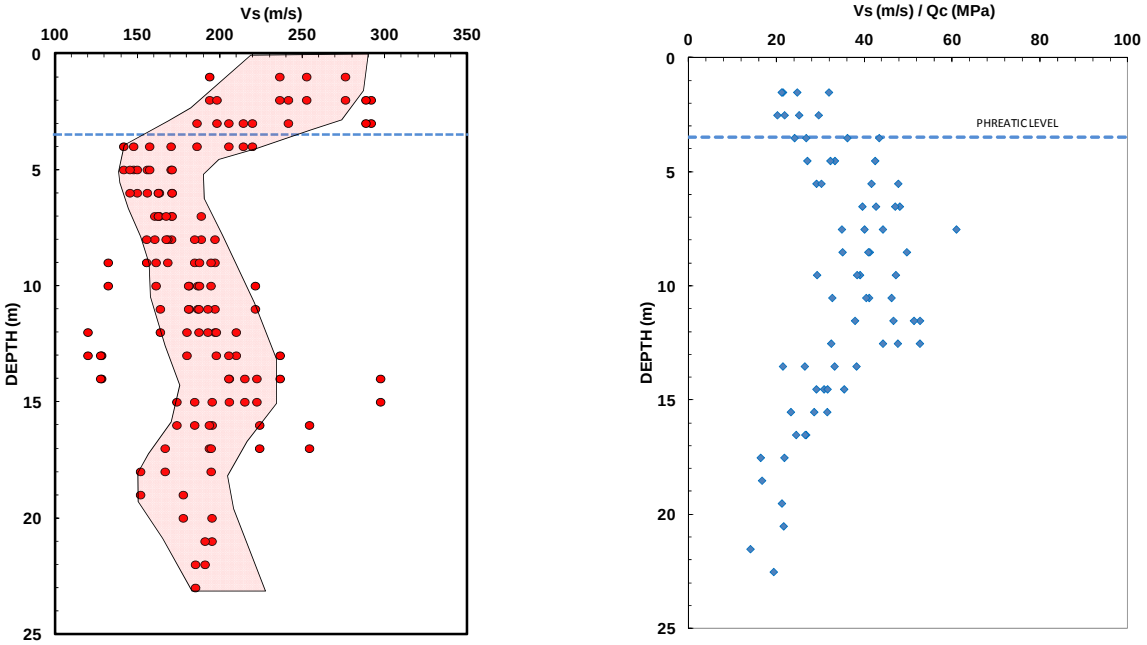

Figures 14 & 15: Wave (S) velocity obtained from SCPTU and variation of Vs/Qc, versus depth

4. PRELOADING AS GROUND IMPROVEMENT

Several ground improvement alternatives were considered, including dynamic compaction, vibrocompaction, jet-grouting and preloading. Preloading was selected as the most efficient treatment in this case. It has the advantages that it reproduces the stress state that the foundation is going to have in service and, given the limited amount of fines in this case, it was expected to be a fast treatment with limited waiting times. In addition, in this case, the material used for preloading in the first tank could be "reused" for the second one.

4.1. Representative cross section

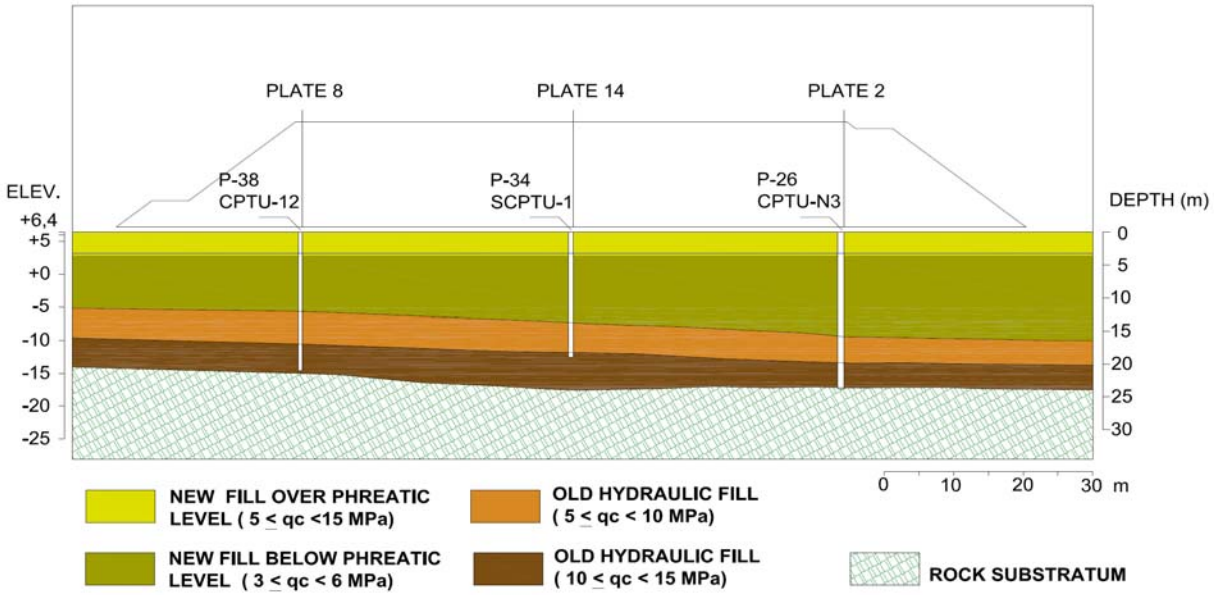

Figure 16: Representative cross-section under Tank 1

4.2. Preload Dimensions

The preloading magnitude has to be equivalent to the load transmitted to the foundation during the hydraulic proof (285 kPa). Since during the earthworks it could be verified that the apparent density was over 20 kN/m^3, the height could be limited to 16 m. The shape of the preloading fill was a conical frustum with a 130 m diameter base and a 80 m diameter top. Photo 2 shows the aspect of the completed preloading.

Photo 2: Completed Preload of Tank Nr 1

4.3. Monitoring

In each tank, the following monitoring has been employed: 14 settlement plates (12 in the perimeter and 2 in the center); 2 sets of extensometers with measurements at three depths, 3 inclinometers with their quadrant oriented towards the adjacent tank. (Piezometers have not been employed given the high permeability of the sands.)

4.4. Results

Figure 17 shows the load (expressed as preloading height) vs settlement curve observed during preloading construction and unloading. Note that during unloading the recovered deformation (upwards movement) during preloading removal was 8,6 times smaller than the settlement during first loading. Figures 18 and 19 show the results of the more inclinometer with the highest deformations, as well as the variation of maximum measured displacements with time and with fill height.

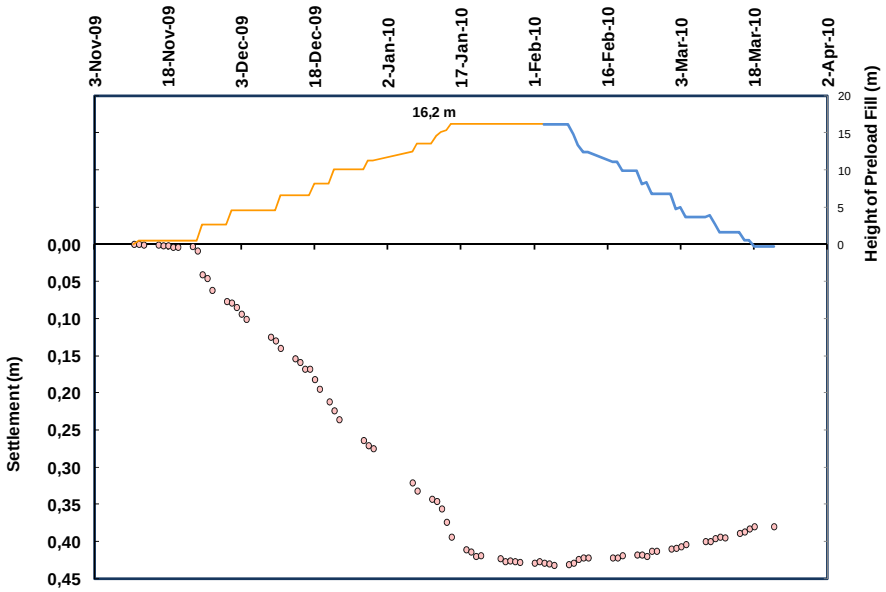

Figure 17: Preload height and settlement vs time

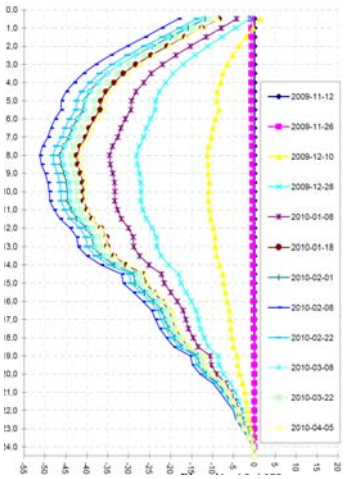

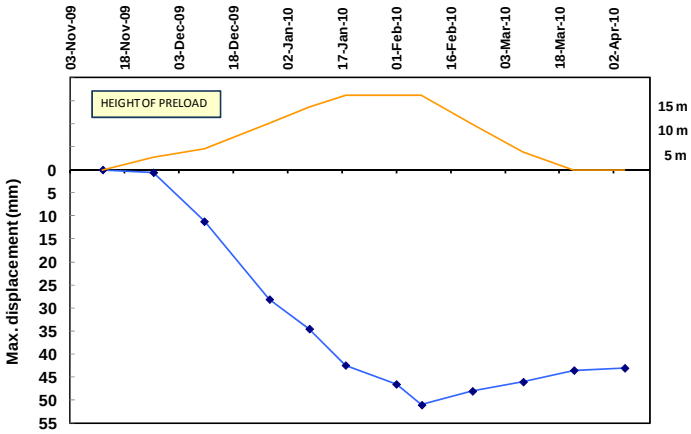

Figures 18 & 19: Results of Inclinometer Nr 1 and evolution of maximum displacement versus time and height of preload.

The deformation moduli of each layer should be proportional to the CPTU tip resistance Qc. The relationship between them has been shown in Figure 20, where to additional lines (representing Em= 3 to 5 Qc) have been presented as well. The upper layer corresponds to the less dense layers, whereas the lower line corresponds to the denser sand levels.

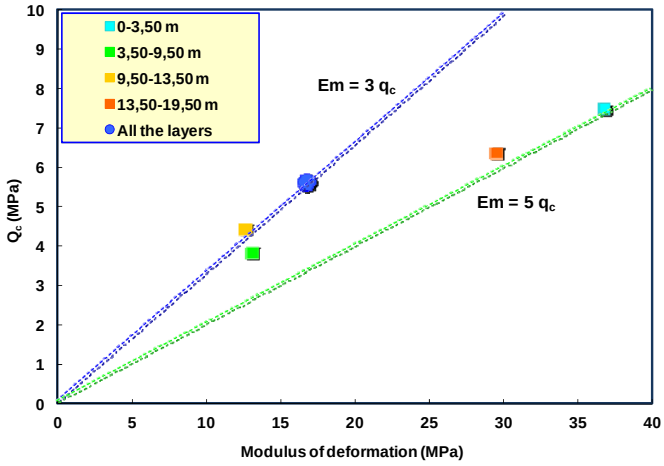

Figure 20: Correlation between Qc and Em

5. SETTLEMENTS DURING CONSTRUCTION OF THE EXTERIOR RING

Figure 21 shows the settlement as the exterior "ring" concrete structure is being constructed. The maximum load once that such ring is constructed will be of 230 kPa acting approximately over a width of 5-6 meters. The observed settlement is being smaller than predicted.

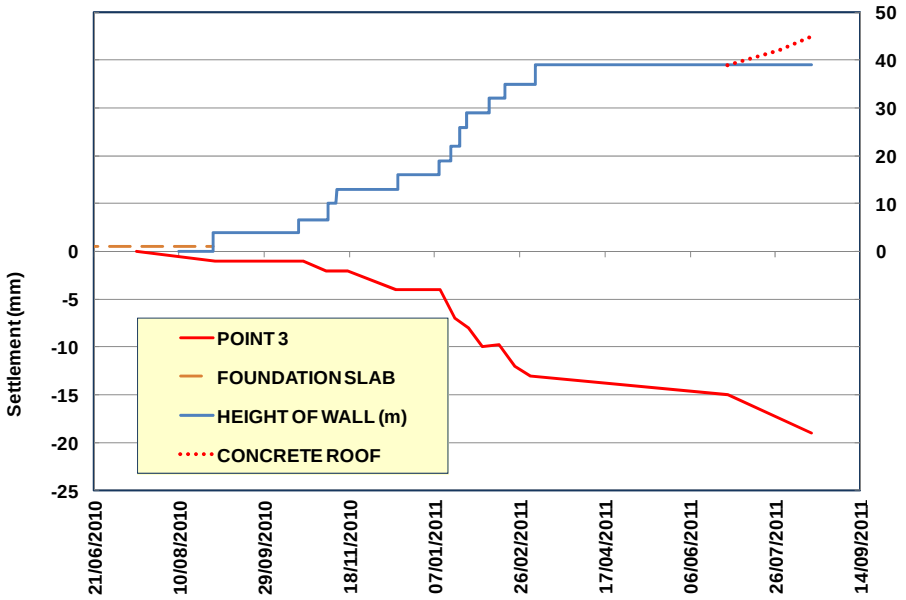

Figure 21: Settlement during the concrete ring construction

6. CONCLUSIONS

A large hydraulic fill has been recently constructed in El Musel (Gijon, Spain) using dredged sands of marine origin from nearby locations. The main purpose of such fill is the construction of industrial facilities for Enagas and, in particular, the construction of two large dimension LNG tanks for a regasification plant.

This article presents the results of the site and geotechnical characterization programs (boreholes, dynamic and static penetration, etc.) and it also presents some correlations that could be established for the available materials in this case.

In addition, we discuss the monitoring details and observed behavior of a preloading scheme that was chosen as a ground improvement alternative for the foundation of the tanks. Preloading has been shown to be an efficient improvement alternative for the tank foundations in this case, with limited settlements during unloading-reloading that are below the accepted thresholds.

7. ACKNOWLEDGEMENTS

FLUOR is the project manager of the works. The main engineering contractor of tanks at the site is a Joint-Venture between DURO FELGUERA and FCC. GEOCISA conducted and managed the site characterization program. Their support, as well as the support of ENAGAS engineering department, is gratefully acknowledged.

REFERENCES

Lee, K.M. (2001). "Influence of placement method on the cone penetration resistance of hydraulically placed sand fills". Canadian Geotechnical Journal. 38(3). pp. 592–607.

Lee, K.M., Shen, C.K., Mitchell, J.K. (1999). "Effects of placement method on geotechnical behavior of hydraulic fill sands". Journal of Geotechnical And Geoenvironmental Engineering (ASCE);125(10). pp. 832–846.

Na, Y.M., Choa, V., The, C.I., Chang M.F. (2005). "Geotechnical parameters of reclaimed sandfill from the cone penetration test". Canadian Geotechnical Journal; 42. pp. 91–109.

Robertson, P.K., Campanella, R.G. and Wightman, A. (1983). "SPT-CPT Correlations". Journ. Of Geotech. Eng. ASCE, 109(11).

Whitman, R.V. (1970). "Hydraulic fills to support structural loads". Journal of the Soils Mechanics and Foundations Division (Proceedings of the American Society of Civil Engineers); 96(SM1). pp. 23–47.